RESEARCH ARTICLE | FEBRUARY 05 2001

Domain structures and planar defects in $SrBi_2Ta_2O_9$ single crystals observed by transmission electron microscopy

Xinhua Zhu; Jianmin Zhu; Shunhua Zhou; Qi Li; Zhiguo Liu; Naiben Ming

Appl. Phys. Lett. 78, 799–801 (2001)
https://doi.org/10.1063/1.1347383

Domain structures and planar defects in $SrBi_2Ta_2O_9$ single crystals observed by transmission electron microscopy

Xinhua Zhu,[a] Jianmin Zhu, Shunhua Zhou, Qi Li, Zhiguo Liu, and Naiben Ming
National Laboratory of Solid State of Microstructures, Department of Physics, Nanjing University, Nanjing 210093, People's Republic of China

(Received 31 May 2000; accepted for publication 14 December 2000)

In this work, the domain structures and structural planar defects in $SrBi_2Ta_2O_9$ (SBT) single crystals with (001) orientation were investigated by transmission electron microscopy. The 90° domain walls are identified by the 90° rotation relationship of the electron diffraction pattern about the [001] zone axis, and which exhibit irregular configurations. Antiphase boundaries (APBs) in SBT single crystals are also observed, which exhibit ribbon-like morphologies. Fourfold vertices formed by four APBs meeting together are observed as predominant singularities, and are explained by a four-state clock model, in which the four states are considered as the TaO_6 octahedra tilting left, right, forward, or backward along the crystallographic directions. Some threefold vertices are also observed since both threefold and fourfold vertices are energetically allowed in the present model. [DOI: 10.1063/1.1347383]

In recent years much attention has been paid to the use of ferroelectric thin films in nonvolatile memory applications. Ferroelectric $SrBi_2Ta_2O_9$ (SBT) thin films have been considered as promising candidates for such devices due to better fatigue properties and lower coercive fields compared to films of the PZT family.[1,2] Various techniques such as pulsed laser deposition,[3] metalorganic chemical vapor deposition,[4] chemical solution deposition,[5,6] and radio frequency sputtering[7] have been used to successfully fabricate SBT thin films. The ferroelectric properties such as fatigue and retention characteristics of SBT thin films have been focused on the nonvolatile memory applications. However, despite the intensive research on physical properties, some basic properties, for example, the ferroelectric domain configurations and mechanism of domain switching, remain unknown. It has only been recently that serious investigations of domain structures have been carried out in these materials in an attempt to correlate the excellent ferroelectric properties with domain structures.[8,9] To better utilize techniques for domain control, more fundamental understanding of the property–domain structure relations in ferroelectrics is urgently needed. In this letter, domain structures and planar defects in SBT single crystals with (001) orientation were investigated by transmission electron microscopy (TEM) and selected area diffraction patterns (SADPs). The 90° domain walls were identified by the 90° rotation relationship of the electron diffraction pattern about the [001] zone axis. Planar defects such as antiphase boundaries (APBs) in SBT single crystals were also observed, which exhibited ribbon-like morphologies. Fourfold vertices formed by four APBs meeting together were observed as the predominant singularities. This is explained by a four-state clock model, in which the four states correspond to four different tilt angles for TaO_6 octahedra. Some threefold vertices were also observed because of both threefold and fourfold vertices being energetically allowed in the four-state clock model.

The SBT single crystal with (001) orientation was grown in a similar manner to that used by Machida *et al.*[9] by adding excess Bi_2O_3 as a flux. The size of the crystal platelet is about 3 mm×3 mm×0.1 mm (in thickness). Specimens for TEM observations were prepared by mechanical polishing to ~30 μm, and then by Ar^+ ion milling at 4 kV with incidence angle of from 15° to 12°. After perforation, the samples were further milled with 3 kV ions with an incidence angle of 10° to remove the surface contamination. The lattice images and planar defects of the SBT crystal were observed by high resolution transmission electron microscopy (HRTEM) (JEOL TEM-4000EX) operated at 400 kV with a double-tilt stage. The domain structures of the SBT single crystal were observed by JEOL JEM-2000EX TEM with a side-entry double-tilt stage.

The displacive ferroelectric SBT is described at room temperature in space group $A2_1am$ as a commensurate modulation of idealized *Fmmm* parent structure derived from an $I4/mmm$ structure.[10] Ferroelectric domain structures in SBT materials can be theoretically investigated by the theory of space groups. The space group of a parent structure of SBT can be chosen as $F4/mmm$ since it has the same size of the unit cell as the ferroelectric structure $A2_1am$. There are five kinds of possible domain walls in SBT materials, which are antiphase boundaries, 180° domain wall, 90° domain wall, APBs combined with 180° domain wall, and APBs combined with 90° domain wall, respectively.[11] In this work, we will focus on the TEM investigations on 90° domain walls and APBs in SBT crystals with (001) orientation.

To examine the SBT single crystal orientation, we first obtain the [001] zone-axis selected area electron diffraction pattern and the related HRTEM lattice images of the SBT single crystal, as shown in Fig. 1. It is clear that the 0.277 nm (d_{200} or d_{020} value) lattice fringes can be resolved, and the lattice parameters of a and b axes were determined to be

[a]Electronic mail: apxhzhu@polyu.edu.hk; present address: Department of Applied Physics, The Hong Kong Polytechnic University, Hung Hom, Kowloon, Hong Kong.

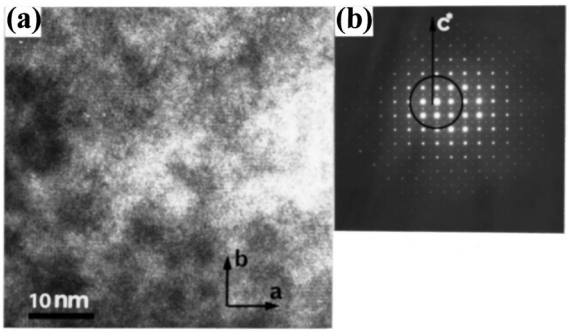

FIG. 1. (a) HRTEM lattice image of SBT single crystal with (001) orientation viewed along [001]; (b) corresponding selected area electron diffraction pattern.

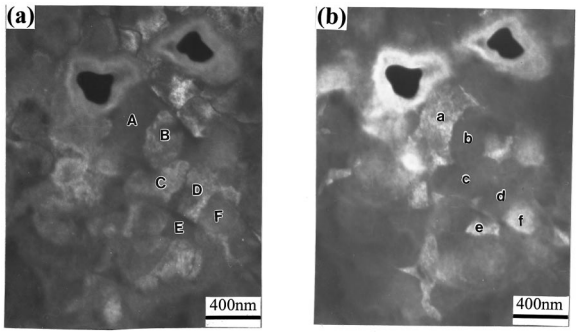

FIG. 3. (a) Dark field image obtained by using weak $(100)_A$ superlattice reflection, and (b) dark field image obtained by using weak $(100)_B$ superlattice refraction. The bright and dark regions, which are reversed in the two images are separated by 90° domain walls.

0.554 nm. This value is in agreement with that refined by x-ray and electron diffraction.[10] That also confirmed that the SBT single crystal was (001) orientation.

Ferroelectric 90° domains in an SBT crystal with (001) orientation were examined by TEM dark field technique and selected area diffraction patterns. The [001] zone-axis selected area diffraction patterns taken from two single domains A and B in the SBT single crystal are shown in Figs. 2(a) and 2(b), respectively. It is observed that the two SADPs are rotated around the [001] direction with respect to each other by 90°. Figure 2(c) shows a SADP pattern taken from a domain wall. This pattern is the superposition of two [001] diffraction patterns, which are rotated around the zone axis with respect to each other by 90°. That indicates the presence of 90° domain walls, as shown in Fig. 3. Figures 3(a) and 3(b) are the dark field TEM images, obtained by using weak $(100)_A$ and $(100)_B$ superlattice reflections marked in Fig. 2(c), respectively. Since each reflection originated from either domain only, the domain that does not contribute the relevant reflection should exhibit dark contrast

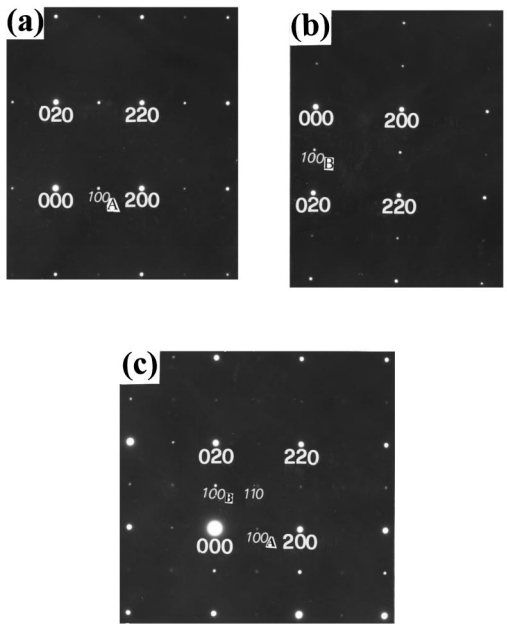

FIG. 2. (a) [001] zone-axis selected area diffraction patterns of single domain A, (b) single domain B, and (c) around a domain wall, in which two [001] zone-axis selected area diffraction patterns with 90° rotation relationship are observed.

in the dark field image. It can be observed that the contrast of several areas marked by A, B, C, D, E, and F in Fig. 3(a) is reverse to that corresponding areas as marked by a, b, c, d, e, and f in Fig. 3(b). Therefore the bright and dark regions, which are reverse in these two images such as A and B marked in Fig. 3(a) should form 90° domain walls. It is observed in Fig. 3 that the morphologies of domains in SBT single crystal appear granular. The origin of which can be explained that the simultaneous nucleation of a large number of domains occur when an SBT single crystal is cooled below the Curie temperature, and the granular-shaped domain formation is beneficial to reducing the free energy of the single crystal. Obviously, the free energy of a state with complicated domain structures is much lower than that of the single domain state. In the present observation, the 90° domain walls exhibit irregular configuration. A similar result was reported in SBT ceramics.[12] From the TEM image, it seems as if the SBT single crystal sample appears granular morphology. That is an artifact of the image conditions used to identify the ferroelectric domains. Actually the SBT single crystal is a thin platelet about $3\ \text{mm}\times 3\ \text{mm}\times 0.1\ \text{mm}$. The surface ($3\ \text{mm}\times 3\ \text{mm}$) of the platelet is very smooth, which is confirmed by the atomic force microscopy image. The smooth surface of this platelet is thought to be a *c* plane from the (001) orientation in the x-ray pattern and crystalline anisotropy.

An APB is a wall that separates two domains of the same ordered phase. It results from symmetry breaking that occurs during ordering processes, which can start at different locations on a disordered lattice. An APB forms when two such regions contact so that they display wrong compositional bonds across the boundary. The contrast of APB is influence by the displacement of vector **R** at an APB, the Bragg reflection **g** of the ordered structure, and its structure amplitude $F(\theta_g)$. The APB obeys precise extinction contrast rules: a given APB is out contrast if the condition $\mathbf{g}\cdot\mathbf{R}=0$ modulo 2π is fulfilled; if not, it displays a fringe contrast. Therefore, the images of APBs are only observed with the superlattice reflections but not with the fundamental reflections. Since, in dynamic conditions, the periodicity of the fringe is correlated to the extinction distance that is at least a few hundred nanometers for a superstructure reflection, the fringes of APBs are reduced to a single dark fringe. Figure 4(a) is a dark field image of APBs in an SBT single crystal with (001) orientation, which was taken with a (120) super-

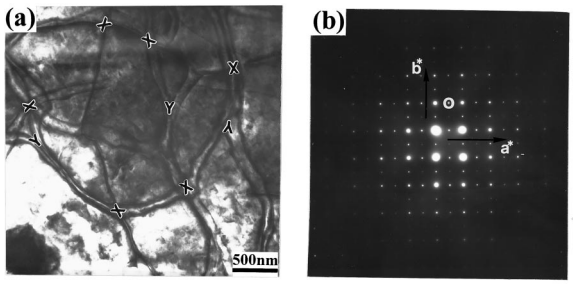

FIG. 4. (a) Dark field images of antiphase boundaries in SBT single crystals taken with (120) superlattice reflection, in which fourfold vertices are marked by dark X, and threefold vertices marked by dark Y; (b) corresponding selected area electron diffraction pattern.

lattice reflection marked by a circle in Fig. 4(b). Figure 4(b) is the corresponding SADP showing the [001] zone of the SBT single crystal. It is observed that the APBs in Fig. 4(a) exhibit ribbon-like morphologies and generally form vertices. It is worth noticing that their contour is very sinuous, meaning that the APB orientation is completely random. These vertices are predominantly singularities at which four APBs meet together to form four-loop vertices as indicated by dark ''X'' in Fig. 4(a), but a relatively small number of threefold vertices are also observed as labeled by dark ''Y.'' To explain the observed vertices, a four-state clock model developed by Srolovitz and Scott[13] was used, in which the four states correspond to four different tilt angles for TaO_6 octahedra. In SBT, the atomic displacements in TaO_6 octahedra along the *b* and *c* axes are cancelled due to the presence of glide and mirror planes, respectively, they do not contribute to the total polarization. Atomic displacements in TaO_6 octahedra along the *a* axis from the corresponding positions in the parent tetragonal structure can cause the ferroelectric spontaneous polarization. Therefore, the *a* axis is the polar axis in SBT.[10] The TaO_6 octahedral rotation about *a* axis of 7.3° in SBT could enhance the ferroelectric polarization of SBT, and the periodic rotations of TaO_6 octahedra about the *a* axis could form the APBs. Similar results were reported in the crystals of barium sodium niobate.[14] By taking analogy between spin states in spin-models and tilting states of TaO_6 octahedra in SBT, we can apply an appropriate spin-model (four-state clock model) to describe the APB structures observed in SBT single crystal. The crystalline symmetry indicating the allowed octahedra tilting requires the model having fourfold-degenerate ground states. The Hamiltonian of the four-state clock model can be written as

$$H = -J\sum_{N,N} \cos(\sigma_i, \sigma_j) = -J\sum_{N,N} \cos\theta_{ij},$$

where the sum is over the nearest-neighbor tilts and $J>0$, σ_i is the tilt at the ith site, θ_{ij} is the angle between the tilt directions of σ_i and σ_j, which is discretized as $2\pi\sigma_i/q$, where q is the degeneracy of the model. In the present model, the q is equal to 4, and θ_{ij} has four possible values of 0, $\pi/2$, $\pi/$, $3\pi/2$. Due to the nature of the interactions and $\cos\theta=0$ ($\theta=\pi/2$) in a four-state clock model, it is implied that there is no change in energy when a boundary between $\theta=0$ and $\theta=\pi$ states is split into two boundaries separating $\theta=0$, $\theta=\pi/2$, and $\theta=\pi$ domains. This result indicates that both threefold and fourfold vertices are energetically allowed, two similarly signed threefold vertices (clockwise or counterclockwise) could attract and combine into together to form a fourfold vertex. To theoretically understand the observed APB microstructures, the simulation on the kinetics of domain pattern evolution can be carried out by a standard Monte Carlo technique. The preliminary results show that APB vertices are predominantly of the fourfold type, and some threefold vertices could be also observed.

In summary, the ferroelectric domain structures in SBT single crystals were examined by TEM observation and selected area diffraction patterns. From the 90° rotation relationship of the electron diffraction of [001] zone axis, the 90° domain walls are confirmed, which demonstrate irregular configurations. Antiphase boundaries in (001)-oriented SBT single crystals exhibit ribbon-like morphologies, and generally terminate in fourfold vertices. A four-state clock model is used to describe the APB structure. Some threefold vertices can be also observed because of both threefold and fourfold vertices being energetically allowed in the present model.

The authors are the recipient of Motorola Semiconductor Products Sector sponsored research. This work is also a part of the research projects funded by the National Natural Science Foundation of China (59832050), the opening project of National Laboratory of Solid State Microstructures (M981308), Nanjing University Talent Development Foundation, and by a grant for State Key Program for Basic Research of China. The authors would like to acknowledge Dr. Peir Chu (Motorola Inc.) and Professor Pengdi Han from the Department of Materials Science and Engineering, University of Illinois at Urbana-Champaign for providing the SBT single crystal in this investigation.

[1] J. F. Scott and C. A. Paz de Araujo, Science **246**, 1400 (1989).
[2] C. A. Paz de Araujo, J. D. Cuchairo, L. D. McMillan, M. C. Scott, and J. F. Scott, Nature (London) **374**, 627 (1995).
[3] S. B. Desu, D. P. Vijay, X. Zhang, and B. He, Appl. Phys. Lett. **69**, 1719 (1996).
[4] T. Li, Y. Zhu, S. B. Desu, C. H. Peng, and M. Nagata, Appl. Phys. Lett. **68**, 616 (1996).
[5] T. Atsuki, N. Soyama, T. Yonezawa, and K. Ogi, Jpn. J. Appl. Phys., Part 1 **34**, 5096 (1995).
[6] J. J. Lee, C. L. Thio, and S. B. Desu, J. Appl. Phys. **78**, 5073 (1995).
[7] H. M. Tsai, P. Lin, and T. Y. Tseng, Appl. Phys. Lett. **72**, 1787 (1998).
[8] A. G ruverman and Y. Ikeda, Jpn. J. Appl. Phys., Part 2 **37**, L939 (1998).
[9] A. Machida, N. Nagasawa, T. Ami, and M. Suzuki, Jpn. J. Appl. Phys., Part 1 **36**, 7267 (1997).
[10] A. D. Rae, J. G. Thompson, and R. L. Withers, Acta Crystallogr., Sect. B: Struct. Sci. **48**, 418 (1992).
[11] J. S. Liu, G. J. Shen, Y. N. Wang, P. Li, Z. G. Zhang, X. B. Chen, F. Yan, H. M. Shen, and J. S. Zhu, Ferroelectrics **221**, 97 (1999).
[12] Y. Ding, J. S. Liu, and Y. N. Wang, Appl. Phys. Lett. **76**, 103 (2000).
[13] D. J. Srolovitz and J. F. Scott, Phys. Rev. B **34**, 1815 (1986).
[14] X. Q. Pan, M. S. Hu, M. H. Yao, and D. Feng, Phys. Status Solidi A **91**, 57 (1985).